Interreg North-West Europe RAWFILL

European Regional Development Fund

Emersons Green Geophysical survey summary

Date: January, 2020

ATRASOL sprl Sustainable Consultant
BAV Bergischer Abfallwirtschaftsverband
British Geological Survey NATURAL ENVIRONMENT RESEARCH COUNCIL
i-CLEANTECH VLAANDEREN enabling the future
LES CHAMPS JOUAULT S.A.S.
LIÈGE université Sciences Appliquées
SAMEN MAKEN WE MORGEN MOOIER OVAM
SPAQuE.be

SUBJECT:	**Selected geophysical survey results from Emersons Green**						
☒	report	☐	information	☐	consideration	☐	decision
To:	…			From:	BGS		

Introduction

This report describes the results of the geophysical survey carried out at the landfill in Emersons Green from the 26th to the 28th of July and the 25th to 26th of October 2018. In autumn 2019 the Emersons Green landfill has been completely excavated for housing purposes. This provides us a unique opportunity for direct validation of the geophysical measurements. In the following, we show the results of all geophysical measurements and compare them to the observation which were made during the excavation work.

Summary of the study area

The Emersons Green landfill covered an area of about 23,000 m^2 with a waste thickness of 3 to 5 m. Records indicate that the landfill was operational from 1984 to 1991 during which it mainly accepted inert, industrial/commercial, construction and office wastes including plastics, paper and cardboard. The original topography of the site comprised a valley feature with an ephemeral stream running through it. The host rock is mudstone and sandstone as displayed in Figure 1. The landfill was designed on a dilute and disperse basis (i.e. no engineered leachate or gas management system) and was capped with inert soil and topsoil.

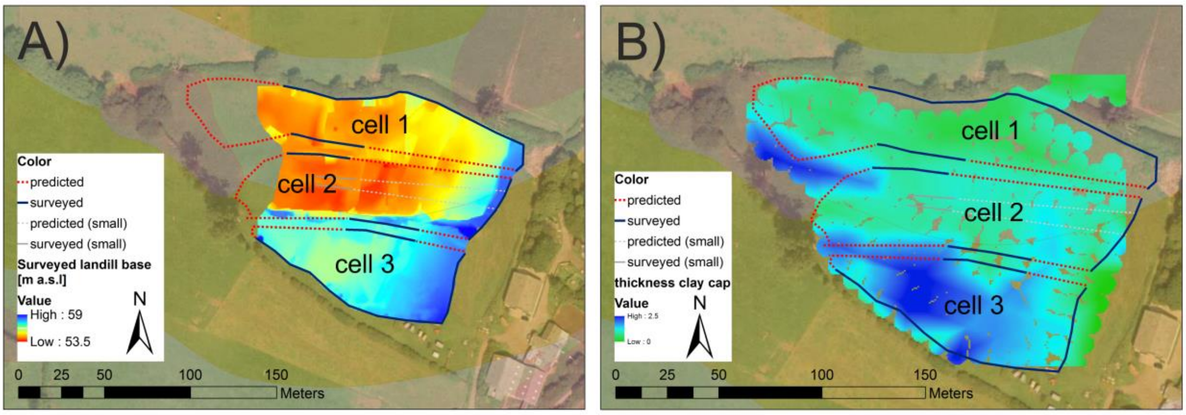

Figure 1: Ground truth information gained during the excavation work at Emersons Green overlain onto the geological map and the satellite image. The clay stanks found during the excavation work, which divide the landfill into three cells are indicated with black and red dashed lines. The surveyed landfill base in (A) shows a thinner waste body in cell 3. The cover layer thickness in (B) shows that cell 3 has a thicker cover layer.

Figure 2 : Clay stanks dividing waste cells were found during the excavations (red arrow).

The following list summarises all the findings during the excavation (compare with Figure 1):

- The landfill was separated into three cells. These cells were excavated into the natural clayey ground and filled with waste. The clay stanks separating the cells were discovered during the excavation (Fig. 2)
- A step in the landfill base between cells 2 and 3 might be associated with the underlying sandstone.
- A thicker clay cap and a thinner waste layer was found on top of cell 3.
- A small clay division was indicated within cell 2 (contaminated with waste).
- The waste composition is a mix of plastic, metal, wood, paper, fabric, inert, etc. with no strong compositional changes across the site.

Geophysical investigation

Geophysical measurements in Emersons Green involved Electromagnetics (EM, in-phase and out-of-phase at four different depths) and Magnetics (Mag, total field and vertical gradient) to map the lateral extent and detect compositional changes within the waste. Electrical Resistivity Tomography (ERT), Induced Polarization (IP) and Multichannel Analysis of Surface Waves (MASW) were applied on several profiles crossing the landfill. These methods are expected to provide more detailed information about vertical extent and compositional changes. The extent and coverage of all methods is summarized in Figure 3.

All geophysical measurements were done on the clayey cover layer after the topsoil layer of about 30 cm thickness was removed (Fig. 3A). In some areas to the north of the landfill, waste was already visible at the surface (Fig. 3C). In June 2018, when all Magnetic, ERT, MASW and the western part of the EM data were acquired, the groundwater level was close to the surface as indicated by a water filled trial pit on the north-eastern end of the landfill (Fig. 3B). During the completion of the EM survey in October 2018, the groundwater level in the trial pit was about 30 cm lower.

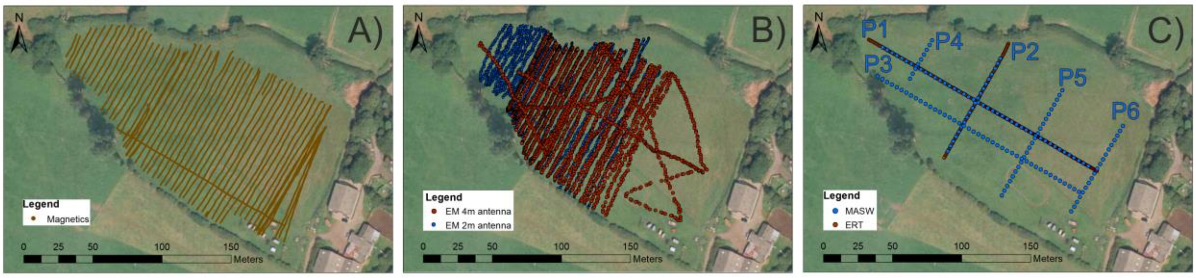

Figure 3: Geophysical survey extent. A) Magnetics was measured on a grid of parallel 4 m spaced lines. B) EM was acquired on a similar grid with 2 to 4 m interline spacing. C) ERT was deployed along two perpendicular profiles across the landfill which coincided with MASW measurements. Four additional MASW profiles were acquired parallel to the other profiles.

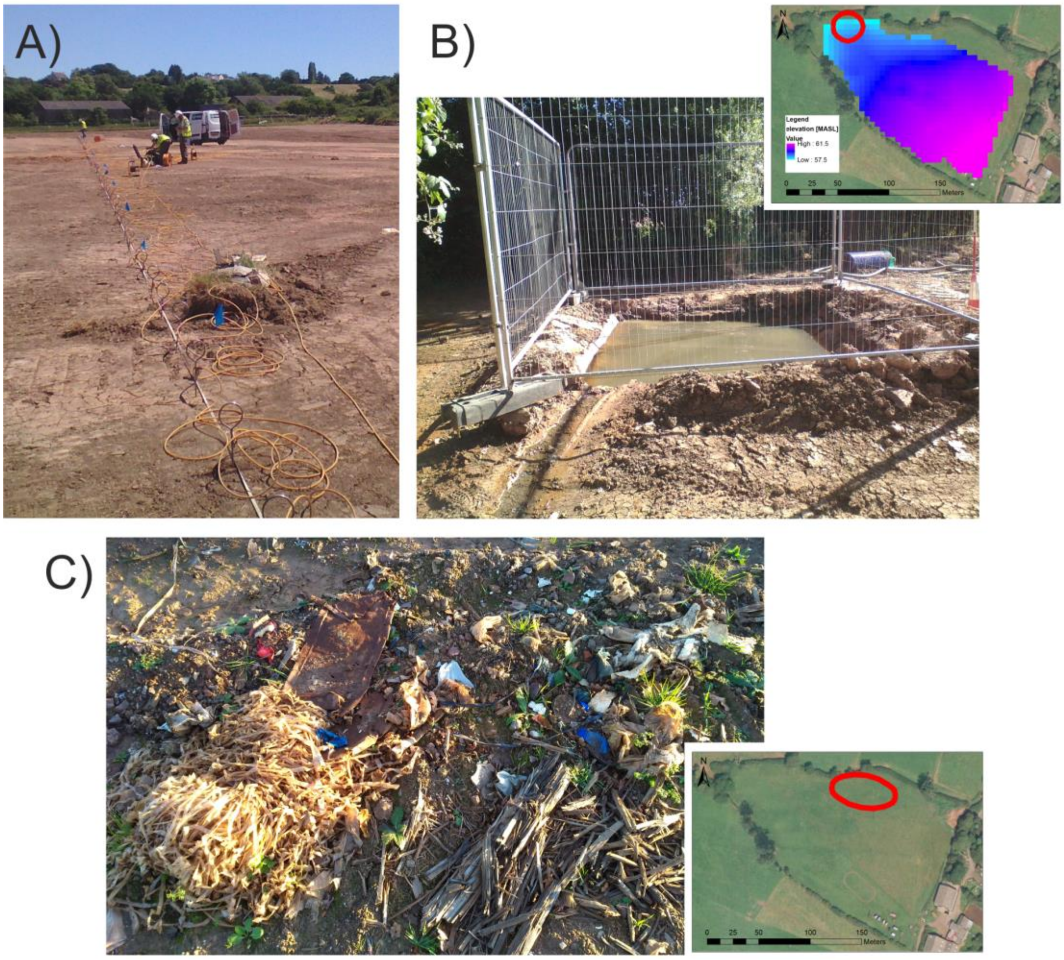

Figure 4: Conditions during the geophysical survey. A) The survey was done on the clayey cover layer after the topsoil was removed. B) The groundwater level during the measurements in June 2018 was high as indicated by a trial pit on the north-eastern side of the landfill. In October 2018, the water table in the trial pit was about 30 cm lower. C) At some locations in the northern part of the landfill, waste was visible at the surface.

Geophysical processing

For the EM and the Mag, all data were interpolated to produce maps. The ERT and IP were pre-processed by filtering based on reciprocal errors and inverted with Res2DInv. The MASW was processed with the SurfSEIS software. All geophysical results were spatially compared with the findings of the proceeding excavations on site.

Geophysical Survey results

Electromagnetic mapping

The results of the Electromagnetics measurements are displayed as maps in Figures 5 and 6. These maps display the apparent conductivities (Fig. 5) and the magnetic susceptibility (Fig. 6) at four different depths below surface corresponding to the depths of maximum sensitivity of the specific EM antenna configuration (2m or 4m antenna, vertical or horizontal orientation). Thus it has to be noted that the displayed values are influenced by the conductivity distribution in the lateral vicinity and vertically above these depths.

Figure 4a shows two very distinct areas of increased conductivities, whose conductivity decreases with depth until disappearing at 6 m (Fig. 4b to d). A third less pronounced area of increased conductivity is seen adjacent to the South at 2.5 m depth (Fig. 4b). In general, waste material is associated with high conductivities (Soupios and Ntarlagiannis, 2017). Thus, the areas of higher conductivities perfectly reveal the three-cell landfill structure which was discovered during the excavations. Cell three only appears at deeper depth due to the thicker cover layer in the South. In addition, since the low conductivities patches have disappeared in Figure 4d, the electrical conductivities indicate that the landfill base must be above or around 6 m below the surface. The small clay stank in cell 2 whose location is indicated by the grey lines in Figure 1, can't be identified on the conductivity maps. This might be due to its contamination with waste. Regarding waste composition, it is difficult to draw conclusions since the measured conductivity and the magnetic susceptibility are influenced by changes of the cover layer thickness (Dumont et al., 2017). Thus, the lower amplitudes of the magnetic susceptibility in cell 3 as seen in Figure 5 might not only be caused by a lower content of metallic material but might be damped due to the thicker cover layer.

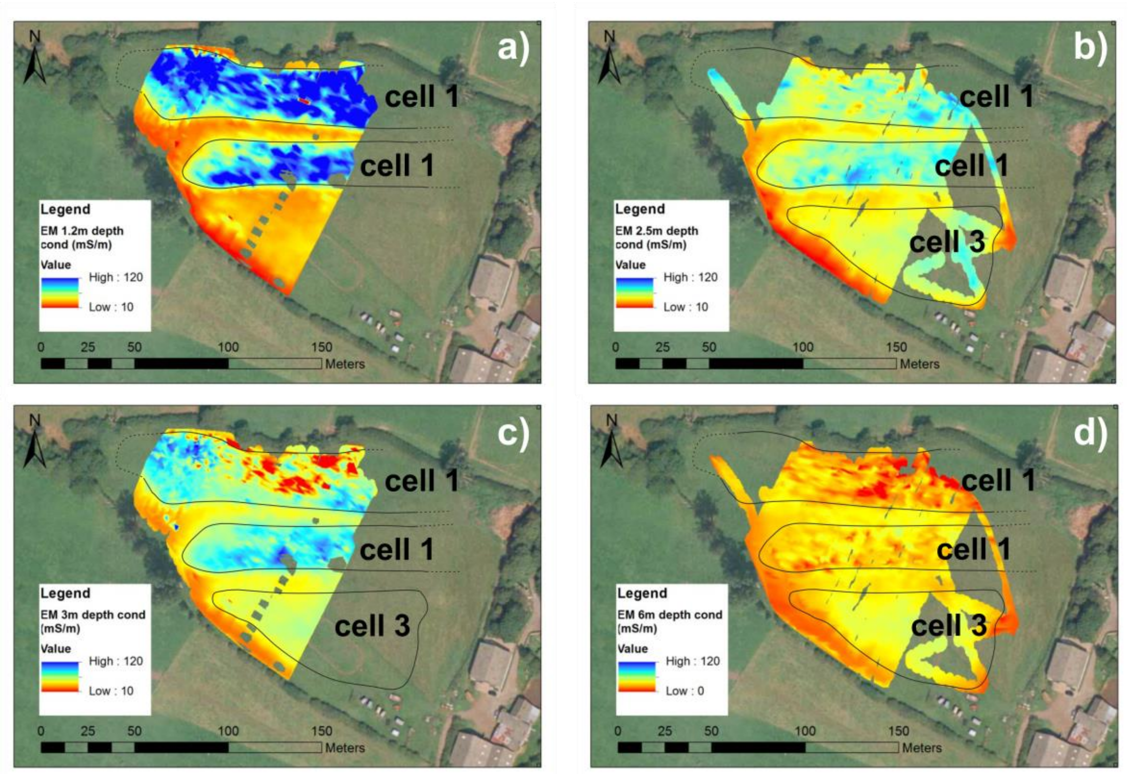

Figure 5: Electrical conductivity map corresponding to the following depths: a) 1.2m, b) 2.5m, c) 3m and d) 6m. The cell-type structure is clearly indicated by patches of higher conductivities.

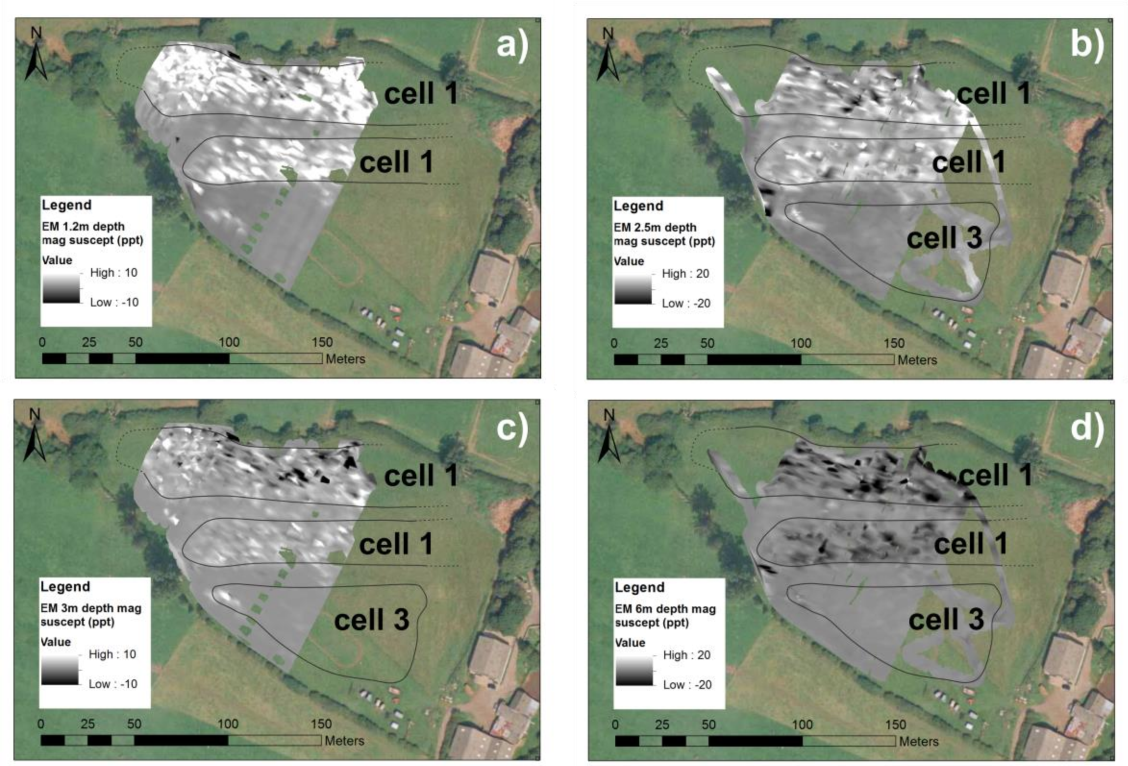

Figure 6: Magnetic susceptibility maps corresponding to the following depths: a) 1.2m, b) 2.5m, c) 3m and d) 6m. The two northern cells are indicated by higher amplitudes of magnetic susceptibility this could be caused by a higher metal content and/or the thinner cover layer thickness.

Magnetic mapping

The Magnetics maps displayed in Figure 6 show similar indications as seen from the EM results. Since the magnetometer measures the earth magnetic field, the cover layer thickness has a lower impact on the measurements but the underlying geology in contrast could influence the measurements (Dumont et al., 2017). However, the total magnetic field and the vertical gradient maps clearly indicate the cell-type structure seen in the EM data (black arrows in Figs. 2a and b). In addition, the magnetic gradient map in Figure 2b reinforces that cells 1 and 2 contain an increased amount of metallic material.

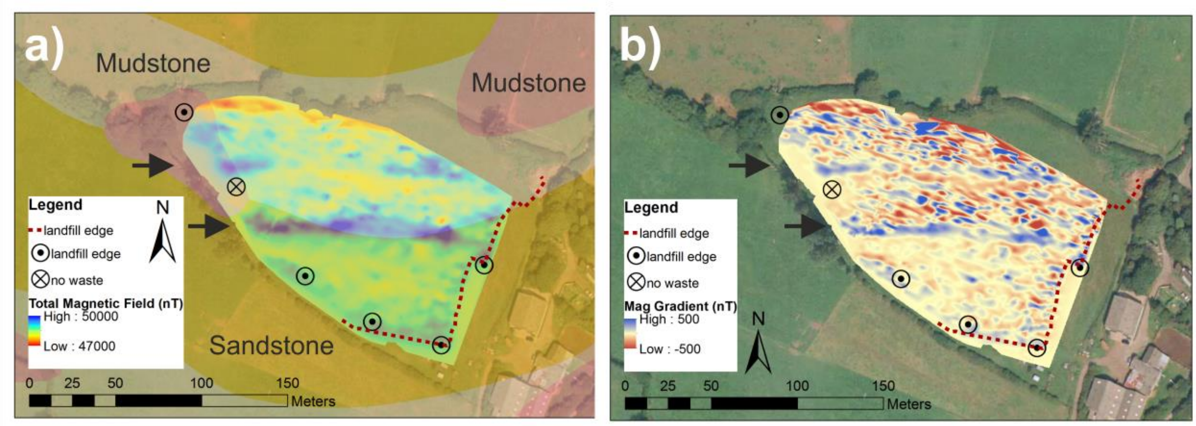

Figure 7: Magnetics data displayed as total magnetic field (a) and vertical gradient (b). The geology displayed in (a) has no visible influence on data. Distinct East-West aligned features, corresponding to the waste cell boundaries, are visible as indicated by black arrows. The vertical gradient indicates a higher metal content in the northern two cells.

Electrical resistivity (ERT) and IP

Figure 8 displays the results of the two profiles measured with IP and ERT. The IP profiles show areas of increased chargeability which matches very well with the trial pit logs and the lower waste boundary found during the excavation (white line). This clear high chargeability signature of the waste is caused by a relatively high content of metallic scraps, organic material (Aristodemou, 2000) or wood or plastic sheet layering (Carlson, 2001). Similarly, the cell-type structure is well represented in the IP data with a thicker cover layer and a decreased chargeability at the position of the clay dams dividing the cells (grey dotted delineation).
The ERT data, in contrast, seems not to be in accordance with the cell-type structure. An explanation for this could be that the ERT measurements are heavily influenced by the moisture/leachate content with the consequence that there is no resistivity contrast between the saturated waste and the mudstone underlying cells 1 and 2. In terms of geology, the ERT detected the top of the sandstone (black dotted lines).

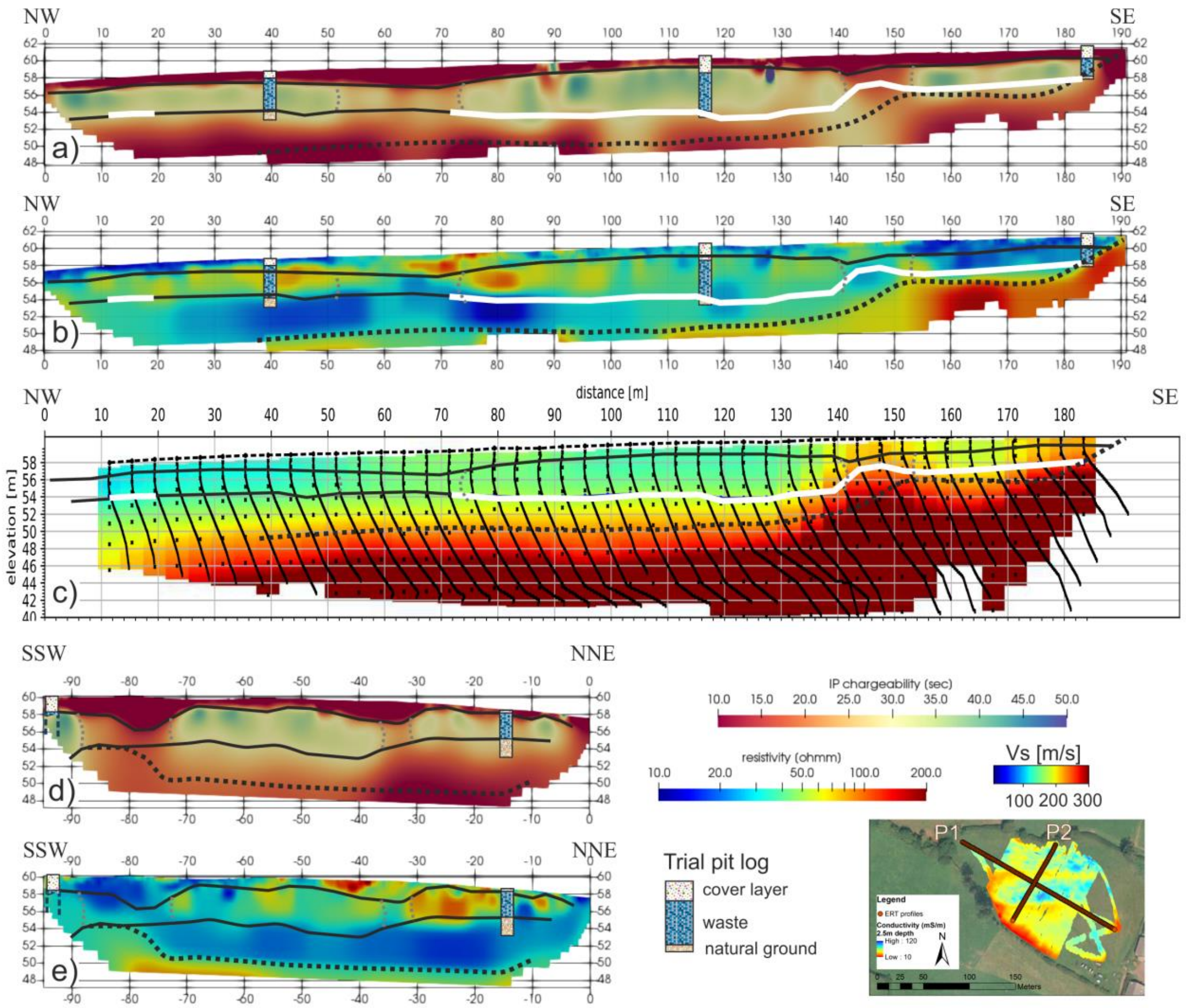

Figure 8: Comparison of the IP, ERT and MASW data along two perpendicular profiles whose location is shown on the bottom right map. a & d) Chargeability along P1 and P2 (IP data). b & e) Resistivities along P1 and P2 (ERT data). C) MASW data along P1. The shear wave velocities are represented by the colour scale. The vertical black lines represent the normalized 1D-velocity-depth profiles at their respective position along the profile.

MASW

Figure 9 provides an overview of all measured MASW profiles. A clear layered structure is seen with low velocity on top and a layer of increased velocity at depth. Figure 7c which displays profile P1 in more detail, clearly shows that the waste body corresponds to low velocities. The black, vertical aligned lines in the figure represent the normalized 1D-velocity-depth profiles at their respective location along the profile. It can be clearly seen that in addition to the low velocity of the waste, there is very little increase in velocity with depth within the waste layer. The depth where the velocity starts increasing matches the discovered bottom of the waste layer very well (indicated by a white line). This is more pronounced at the south-eastern end where the waste is underlain by sandstone causing a bigger velocity contrast than towards the north-western end where the waste is underlain by mudstone.

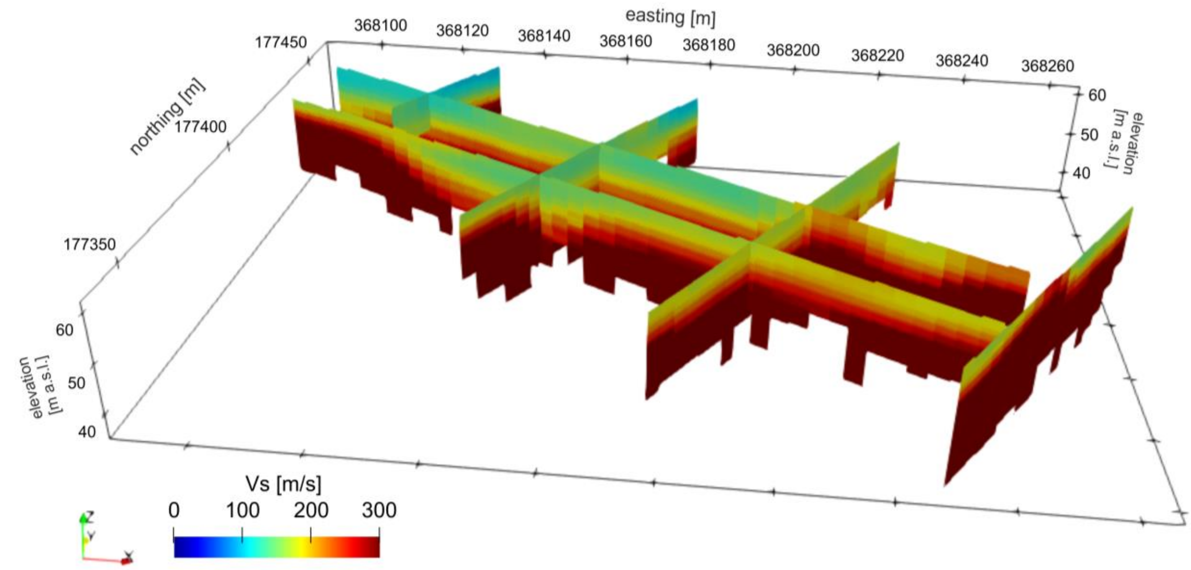

Figure 9: Profiles displaying the shear wave velocity derived from the MASW measurements.

Conclusion

EM and Magnetic mapping were able to provide a rapid overview of the landfill structure. IP was the most suitable method to delineate the extent of the waste layer whereas ERT seems more sensitive to changes in moisture/leachate content. MASW was able to correctly estimate the landfill base. This study clearly shows that a multi-method geophysical approach in combination with targeted sampling is essential to avoid misinterpretations. Furthermore, planning the profile location of the more time-consuming methods such as IP, ERT and MASW based on the results of the rapid mapping methods such as EM and Mag can improve the survey efficiency.

References

Aristodemou, E., Thomas-Betts, A., 2000. DC resistivity and induced polarisation investigations at a waste disposal site and its environments. Journal of Applied Geophysics, 44: 275–302.

Carlson, N.R., Hare, J.L., Zonge, K.L., 2001. Buried landfill delineation with induced polarization: Progress and problems, in: Symposium on the Application of Geophysics to Engineering and Environmental Problems (SAGEEP).

Dumont, G., Robert, T., Marck, N. and Nguyen, F., 2017. Assessment of multiple geophysical techniques for the characterization of municipal waste deposit sites. Journal of Applied Geophysics, 145: 74-83.

Soupios, P., Ntarlagiannis, D., 2017. Characterization and Monitoring of Solid Waste Disposal Sites Using Geophysical Methods: Current Applications and Novel Trends. In: A.S. Sengupta D. (Editor), Modelling Trends in Solid and Hazardous Waste Management. Springer, Singapore, pp. 75-103.

Contact

Feel free to contact us.

Local contact details:

BELGIUM	ATRASOL	renaud.derijdt@atrasol.eu
	i-Cleantech Vlaanderen/VITO	alain.ducheyne@vito.be
	OVAM	ewille@ovam.be
	SPAQuE	c.neculau@spaque.be
	Université de Liège	f.nguyen@ulg.ac.be
FRANCE	SAS Les Champs Jouault	champsjouault@gmail.com
GERMANY	BAV	pbv@bavmail.de
THE UK	NERC	jecha@bgs.ac.uk

Coordination office:

BELGIUM	SPAQuE Boulevard Maurice Destenay 13, 4000 Liège	c.neculau@spaque.be